Reduced mitochondrial transcription sensitizes acute myeloid leukemia cells to BCL-2 inhibition

Short title: Inhibition of mtDNA expression to treat leukemia

Authors

Laleh S. Arabanian[1], Jenni Adamsson[2], Anke Unger[4], Raffaella Di Lucrezia[4], Tim Bergbrede[4], Arghavan Ashouri[1], Erik Larsson[1],Peter Nussbaumer[4], Bert M. Klebl[4,5], Lars Palmqvist[2,3,*], Claes M. Gustafsson[1,3*,†]

Affiliations

[1] Department of Medical Biochemistry and Cell Biology, University of Gothenburg, Gothenburg, Sweden

[2] Department of Laboratory Medicine, University of Gothenburg, Gothenburg, Sweden.

[3] Department of Clinical Chemistry, Sahlgrenska University Hospital, Gothenburg, Sweden

[4] Lead Discovery Center GmbH, Otto-Hahn-Str. 15, D-44227 Dortmund, Germany

[5] The Norwegian College of Fishery Science, UiT The Arctic University of Norway, PO Box 6050 Langnes, N-9037 Tromsø, Norway

[*]Corresponding authors: lars.palmqvist@clinchem.gu.se and claes.gustafsson@medkem.gu.se

†Lead Contact

Abstract

Overcoming drug-resistance and the subsequent relapse that often occurs with monotherapy is crucial in the treatment of acute myeloid leukemia. We here demonstrate that therapy-resistant leukemia initiating cells can be targeted using a novel inhibitor of mitochondrial transcription (IMT). The compound inhibits mitochondrial RNA polymerase activity and sensitizes the resistant population to the induction of apoptosis. *In vitro* studies on acute myeloid leukemia cells demonstrate that IMT prevents cell proliferation, and together with a selective BCL-2 inhibitor, venetoclax, induce apoptosis and suppress oxidative phosphorylation (OXPHOS) synergistically. AML mouse models treated with IMT in combination with venetoclax show prolonged survival in venetoclax-resistant models. Our findings suggest that certain therapy-resistant leukemia cell populations display a unique dependency on mitochondrial transcription and can be targeted with IMT.

Teaser

Leukemia cells resistant to standard treatment are sensitive to a recently developed inhibitor of mitochondrial gene expression.

42 **Introduction**

43 Acute myeloid leukemia (AML) comprises a devastating and heterogeneous group of diseases,
44 for which patient survival rates have remained stagnant over the last several decades. There is
45 no one standard AML treatment as it depends on the individual situation of each patient.
46 Current cares are focused on allogenic stem cell transplantation as well as patient stratification
47 and therapy selection based on genetic aberrations. These lead to cures in only a fraction of
48 AML patients, highlighting the critical need to develop different approaches. The anti-
49 apoptotic molecule BCL-2 has been a therapeutic target in lymphoid and myeloid leukemia, as
50 in many cancers overexpression of BCL-2 results in dysregulation of apoptosis (*1*). ABT-199
51 (venetoclax), is a specific BH3-mimetic that causes apoptosis by preventing BCL-2 from
52 binding pro-apoptotic BAX and BAK1 proteins (*2*). However, complete responses occur in just
53 ~20% of AML patients treated with Venetoclax (*3*). In addition, many patients relapse, with
54 regrowth initiated by therapy-resistant leukemic clones, suggesting that single agent
55 administration is unlikely to yield lasting responses in most cases. Venetoclax is therefore used
56 in combination with conventional therapies. Together with hypomethylating agents,
57 Venetoclax is now standard of care for patients deemed unfit for intensive induction therapy
58 (*4*).

59

60 Resistance to venetoclax may result from overexpression of the anti-apoptotic proteins MCL1
61 or BCL2L1 (*5*), or through changes in levels of other anti-apoptotic molecules (*6*). Aberrant
62 pro-survival regulation can also be achieved by inactivation of TP53 function, which controls
63 many aspects of apoptosis (*6, 7*). MCL1-dependent resistance to venetoclax can be overcome
64 when the compound is combined with the MDM2 inhibitor RG7388, which causes p53
65 activation. A combination of BCL-2 inhibition and TP53 activation may thus provide an
66 interesting therapeutic approach for treatment of AML (*8*).

67

68 Other combination approaches that promote apoptosis may also be of interest. The majority of
69 ATP required for leukemia stem cell (LSC) function is generated by oxidative phosphorylation
70 (OXPHOS) (*9, 10*). Interestingly, venetoclax-resistant leukemic cells display increased levels
71 of OXPHOS and are protected from mitochondrial stress (*7*). These data suggest approaches
72 to specifically target OXPHOS in leukemia may be an attractive option. In support of this
73 notion, inhibition of mitochondrial protein translation by antibiotics that reduce OXPHOS
74 capacity results in a selective cytotoxic effect on leukemic cell when used in combination with
75 thyrosine kinase inhibitors (*11*). Furthermore, LSCs from *de novo* AML patients display a
76 unique dependency on amino acid metabolism to fuel OXPHOS. When venetoclax is combined
77 with the hypomethylating agent azacytidine, the two compounds act in concert to inhibit amino
78 acid uptake, leading to a drop in OXPHOS and thus cell death (*12*). More recently, AML
79 therapy using a combination of cytarabine (AraC) and venetoclax has highlighted the central
80 role of mitochondrial adaptation during treatment (*10, 13*), indicating the need for a
81 mitochondrial directed combination therapy for AML. Such a therapy may help to overcome
82 existing treatment resistance.

83

84 Recently we developed novel, first-in-class inhibitors of mitochondrial transcription (IMTs)
85 (*14*). IMT treatment specifically targets mitochondrial RNA polymerase (POLRMT) and
86 reduce transcription of mitochondrial DNA, which codes for thirteen key components of the
87 OXPHOS machinery, including subunits of respiratory complexes I, III, IV, and the ATP
88 synthase. As a consequence, IMT treatment impairs OXPHOS system biogenesis in a dose-
89 dependent manner, and decreases cell viability in various tumor cells. Surprisingly, several
90 weeks of per oral IMT treatment is well tolerated in mice and does not cause toxicity in normal
91 tissues, despite inducing a strong anti-tumor response in human cancer xenografts (*14*).

92

93 Here we examine AML cell lines for their sensitivity for treatment with IMT. We find that a
94 combination of IMT and venetoclax displays a synergistic on cell growth and induction of
95 apoptosis. We demonstrate that the efficacy of this approach in leukemia mouse models
96 generated by human AML cell lines as well as primary samples from AML patients.

97

98

99 **Results**

100 **Synergistic effect of IMT in combination with venetoclax on AML cell lines**

101 We were curious whether our inhibitors of mitochondrial transcription (IMTs) (*14*) could be
102 effective against AML cells. The coumarin class of IMTs was optimized by medicinal
103 chemistry to generate lead IMT compounds with improved metabolic stability in mice, such as
104 LDC204857, herein simply referred to as IMT (Fig 1A, Fig. S1 and Table S1). IMT is a close
105 analog of previously described IMT1B (Fig. S1) with a highly similar biochemical and cellular
106 inhibition profile (*14*). It shows an extended half-life *in vivo* due to its increased metabolic
107 stability (Table S1). Thus, by using IMT we could consistently reduce the mouse dose to 50
108 mg/kg per oral once daily, which is very well tolerated and does not exert any adverse effects
109 in mice.

110

111 Using four AML cell lines with different expression of TP53 (MV4-11 and MOLM-13
112 expressing wild type TP53; THP-1 and KG-1 expressing mutated TP53), we monitored the
113 effects of increasing concentrations of IMT on cellular growth using a luminescence-based cell
114 viability assay. Only marginal effects were observed after a 72-h period of exposure to IMT,
115 but all cell lines displayed dose-dependent antileukemic activity after 144 h of treatment (Fig.
116 1B), in line with our previous observations (*14*). We also monitored venetoclax sensitivity by
117 assessing cell viability, and noted that, in line with published work (*15*), a dose-dependent
118 reduction in cell growth occurs after three days and becomes more pronounced after 6 days
119 (Fig. 1B).

120

121 To then investigate whether IMTs show a synergistic effect when combined with venetoclax,
122 we conducted a combination study in AML cell lines (Fig. 1C). After six days of treatment, we
123 found a clear synergistic effect on cell proliferation in MV4-11 and MOLM-13 cell lines, which

124 express wild type TP53, as determined by combination analysis (Bliss-independence model
125 (*16*)). Treatment of THP-1 and KG-1 cell lines, which harbor mutated TP53, only revealed a
126 synergistic effect when using higher concentrations of both IMT and venetoclax (Fig. 1C,
127 additional treatment data are shown in Fig. S2).
128
129 **Combination of IMT and venetoclax synergistically induces apoptosis and loss of**
130 **mitochondrial membrane potential in MV4-11 and MOLM-13 cells**
131 To investigate the factors involved in the inhibition of cell growth with IMT and venetoclax,
132 AML cell lines were treated with single agents (IMT or venetoclax) or a combination of the
133 two (Fig. 2A), and the stages of apoptosis were monitored using Annexin V and PI staining.
134 No detectable increase in apoptosis was induced by IMT exposure alone in any AML cell line.
135 Venetoclax treatment resulted in both early and late apoptosis induction in MV4-11 and
136 MOLM-13 cell lines, and employing a combination of IMT and venetoclax significantly
137 enhanced apoptosis induction in these wild type cell lines. On the other hand, combination
138 treatment did not induce apoptosis in THP-1 and KG-1 mutated cell lines (Fig. 2A).
139
140 One distinctive feature of apoptosis is the disruption of mitochondrial function, which can be
141 measured as loss of mitochondrial membrane potential due to membrane depolarization. As a
142 combination of IMT and venetoclax could synergistically induce apoptosis, we were curious
143 whether combination drug treatment thus affects mitochondrial membrane potential. We
144 observed that venetoclax-sensitive cell lines (MV4-11 and MOLM-13) showed a dramatic loss
145 of mitochondrial membrane potential when treated with both venetoclax and IMT (Fig. 2B).
146 On the other hand, mitochondrial membrane potential in THP-1 cells was not affected by single
147 nor by combination treatment. Interestingly, although KG-1 was venetoclax insensitive, the
148 combination treatment significantly enhanced loss of mitochondrial membrane potential (Fig.

149 2B). These data suggest that a combination of IMT and venetoclax is cytotoxic and
150 synergistically induces cell death in sensitive cells, presumably through disruption of
151 mitochondrial function.
152
153 **Combination of IMT and venetoclax significantly suppresses OXPHOS in AML cells**
154 We next studied whether combination treatment with IMT and venetoclax affects OXPHOS in
155 AML cells. OXPHOS was evaluated by determining oxygen consumption rate (OCR) (Fig.
156 3A), which was measured first as basal respiration and then oligomycin (OMY)-induced leak
157 respiration (ATP-linked respiration) after the addition of oligomycin to inhibit ATP synthase.
158 Stepwise carbonyl cyanide m-chlorophenyl hydrazone (CCCP) titrations were subsequently
159 carried out to reach the electron transport chain respiratory capacity state. Finally, antimycin a
160 (AMA) was added to inhibit complex I/III of the electron transport chain and to terminate
161 respiration, allowing for the determination and correction of residual oxygen consumption,
162 which is indicative of non-mitochondrial oxygen consumption (Fig. 3A). We noted that
163 combination treatment significantly inhibits OXPHOS respiration in venetoclax-sensitive
164 MOLM-13 and MV4-11 cells (Fig. 3B). In comparison, OXPHOS levels in venetoclax-
165 resistant THP-1 cells were unaffected in the presence of single compound or combination
166 treatments, confirming that the inhibition we observed is not a general effect of drug treatment
167 (Fig. 3B).
168
169 In normal hematopoietic cells, glycolysis is upregulated when OXPHOS is blocked (*17*). In
170 contrast to normal hematopoietic cells, high energy turnover AML cells rely predominantly on
171 OXPHOS due to poorly regulated metabolic adaptation. To verify the reliance on OXPHOS,
172 AML cells were grown in growth medium supplemented with either glucose or galactose (Fig.
173 3C). Two ATP molecules are produced when cells use glucose for glycolysis, but if galactose

174 is used instead, no ATP is generated (*18*). We observed no significant decrease in the level of
175 ATP production (Fig. 3C) nor in cell counts (Fig. S3A) in the absence of glucose, indicating
176 that glycolysis is not a major source of energy in AML cells. To test whether AML cells use
177 glycolysis under treatment conditions, OCR was measured in the presence or absence of a high
178 concentration of glucose (Fig. S3B). OCR measured for basal respiration was not significantly
179 different with excess amounts of glucose, again indicating the inability of AML cells to switch
180 to glycolysis when OXPHOS is disrupted.
181
182 **Combination of IMT and venetoclax synergistically delays leukemia initiation in cell-**
183 **derived leukemia mouse models**
184 Following the confirmed synergy between IMT and venetoclax in AML cell lines, we
185 proceeded to test the dual inhibition of mitochondrial transcription and BCL-2 in an AML cell-
186 derived xenograft (CDX) transplantation mouse model. First, the pharmacokinetic profile of
187 IMT was determined in plasma, liver, and bone marrow (BM) of mice, 1, 8, and 24 h post-
188 administration (Fig. S4A). As described above (Fig. S1), the IMT mouse PK profile was
189 superior to IMT1B. IMT was detected in all tissues at all time points when administered alone.
190 To determine the concentration of IMT and venetoclax when administered in combination,
191 plasma samples were then collected 8–11 h post-administration of single or combination
192 formulations and the concentrations of IMT and/or venetoclax in samples were measured (Fig.
193 S4B). Values obtained were all within the effective range, as combination treatment did not
194 affect the individual compound concentrations (*14*). For xenograft experiments, NBSGW mice
195 were intravenously transplanted with MV4-11 AML cells (Fig. 4A). Two weeks after
196 transplantation, engraftment of AML cells was confirmed (evaluated by gating on hCD45+
197 population by flow cytometry in peripheral blood). Treatment then began with vehicle, 50
198 mg/kg IMT, 100 mg/kg venetoclax, or a combination of IMT (50 mg/kg) and venetoclax (100

199 mg/kg) (Fig. 4A), dosed as such based on previously published protocols (*14, 18*). The efficacy
200 of treatments was determined by measuring the proportion of transplanted AML cells in
201 peripheral blood and by survival analysis (Fig. 4B). In all treatment groups, the hCD45+
202 population dropped immediately after treatment, and vehicle- and venetoclax-treated mice then
203 exhibited a rapid rebound. In contrast, in IMT-treated mice the increase in leukemic cell
204 proportion was delayed until eight weeks post-transplantation, and in the combination-treated
205 group for to up to 20 weeks (Fig. 4B). These observations correlate with results from survival
206 analysis (Fig. 4C). IMT treatment of MV4-11 transplanted mice significantly delayed the
207 development of leukemia, inducing a 37% increase in median overall survival (57.5 → 79
208 days). Development of leukemia was further delayed by combination treatment to 131% (57.5
209 → 133 days), and the group contained two mice that did not show any disease symptoms after
210 200 days (post-transplantation) when they had to be euthanized according to ethical
211 permissions. Moreover, leukemic cells were not detectable in the BM of surviving mice at the
212 time of termination. All other mice showed symptoms of leukemia and of these, all but one
213 combination-treated mouse had an increased percentage of leukemic cells in BM (Fig. 4D).
214 These results confirm that treatment with a combination of IMT and venetoclax significantly
215 prolongs leukemia progression in mice. Moreover, the general condition of mice such as
216 behavior, fur, mobility and weight, assessed before (week 2) and after treatment (week 5), were
217 not altered in the IMT-, venetoclax-, or combination-treatment groups when compared to the
218 vehicle-treated group (weights shown in Fig. S5B), suggesting that the treatments were well
219 tolerated. As with single IMT therapy (*14*), treatment with combination therapy did not display
220 any evidence of organ toxicity or drug-associated death in the mice (Fig. S5C, D).
221
222 **IMT and venetoclax synergistically decrease the tumor burden and increase the life span**
223 **in an AML-PDX mouse model resistant to venetoclax.**

224 The CDX mouse model demonstrated IMT could sensitize AML cell lines to BCL-2 inhibitors
225 *in vivo*. We next analyzed effects of combination treatment on a more refined *in vivo* model by
226 generating xenografts using AML patient-derived cells (AML PDX). We first tested an AML-
227 PDX mouse model with resistance to venetoclax (AML sample harboring TP53 mutation).
228 Two weeks post-transplantation with AML PDX cells, NSGS mice were orally treated with
229 IMT, venetoclax, or a combination of the two for 21 days (Fig. 5A). The efficacy of the
230 treatments was determined based on the proportion of human AML cells (determined by
231 hCD45+ population). Six out of 10 mice in each group were euthanized immediately after the
232 last compound administration for end-of-treatment analysis. We found that the combination of
233 IMT and venetoclax resulted in significant inhibition of tumor burden in blood, BM, and spleen
234 of treated mice (Fig. 5B). By examining histology sections of BM and spleen, we found that
235 tissues from combination-treated animals contained less engraftment of leukemic blasts than
236 single- and vehicle-treated mice (Fig. 5C). Accordingly, the frequencies of hCD45+ cells in
237 the BM and spleens of the combination-treated group were largely reduced in comparison to
238 other groups (Fig. 5D), and engrafted tumor cells in combination-treated PDX mice showed a
239 lower proliferating percentage in comparison to single or vehicle treated groups (shown by
240 KI67+/hCD45+ immunohistochemistry staining; Fig. 5E). This demonstrates a synergy
241 between IMT and venetoclax in reducing tumor burden.
242
243 To further analyze the cellular effects of the IMT-venetoclax combination treatment, we
244 analyzed transcriptomes of purified viable AML blasts isolated from PDX models at end of
245 treatment (Fig. 6A). We confirmed that combination treatment had a more pronounced effect
246 on gene transcription as compared to single treatments. In agreement with its more pronounced
247 effect on tumor burden, combination treatment suppressed expression of a number of genes
248 involved in leukemogenesis, including MX1, KCTD12, ITGA and RGL1 (Table S2) (*19*).

249

250 We also analyzed survival by monitoring the mice for disease progression and morbidity.
251 Peripheral blood engraftments were analyzed at regular intervals until the appearance of
252 disease symptoms (Fig. 6B and Fig. S6A). The leukemia burden immediately prior to
253 euthanization demonstrated that the cytoreductive effect of the combination treatment persists
254 (Fig. 6B). However, blood count (determined by RBCs and HGB levels) did not vary
255 significantly between experimental groups, nor did the magnitude of splenomegaly or liver
256 weight vary at the time of euthanization (Fig. S6B–D). Interestingly, mice treated with a
257 combination of IMT and venetoclax succumbed to death significantly later than other treatment
258 groups, with a median survival of 112 days vs 96, 99, and 102 days for vehicle-, IMT-, and
259 venetoclax-treated groups, respectively (Fig. 6**C**). Combination treatment thus increases the
260 life span of venetoclax-resistant AML mouse models, demonstrating that IMT can sensitize
261 AML cells towards other therapies.

262

263 **IMT does not affect tumor burden or life span in an AML-PDX mouse model sensitive to**
264 **venetoclax.**

265 For comparison, we also monitored effects of combination treatment on a PDX model based
266 on AML cells sensitive to venetoclax treatment (AML cells harboring FLT3-ITD, NMP1 and
267 DNMT3A). As expected, we observed that venetoclax treatment significantly reduced the
268 tumor burden in the blood and BM of mice. Combination treatment with IMT did not add to
269 this effect (Fig. 7A). By examining histology sections, we found that both BM and spleen
270 tissues from combination- and venetoclax-treated animals contained reduced proportion of
271 leukemic blasts compared to IMT- and vehicle-treated mice (Fig. 7B). White blood counts
272 (WBCs), red blood counts (RBCs), and hemoglobin (HGB) levels were not significantly
273 different across experimental groups (Fig. S7A). Total body and liver weight of PDX mice

274 were very similar in all groups (Fig. S7B, D), but both venetoclax and combination treatments
275 reduced splenomegaly (Fig. S7C).
276
277 The remaining half of mice were used for survival analysis, which involved regular blood count
278 and chimerism analysis until the appearance of disease symptoms (Fig. 7C). Both venetoclax
279 and IMT caused a modest increase in life span, but combination treatment did not offer an
280 additional effect (Fig. 7D).
281
282
283
284

285 **Discussion**

286 In recent years, the genetic complexity and heterogeneity of leukemia cell populations has
287 become apparent (*20, 21*) and developing effective strategies to target human leukemia
288 initiating cells has thus proven to be a challenging task. Currently, there is considerable interest
289 in therapies, such as venetoclax, that can restore normal apoptosis of cancer cells by directly
290 interacting with the BCL-2 family of proteins. These are effective for some leukemias, but
291 many patients eventually become refractory to treatment and ultimately succumb to their
292 disease (*22, 23*). It has become increasingly important to determine which biological properties
293 are relatively consistent in LSC populations irrespective of genetic makeup (tumor population).
294 Recent observations indicate that several cancer cell types, including LSCs, are reliant on
295 OXPHOS for metabolism (*24*), making inhibition of mitochondrial function a promising
296 therapeutic strategy for AML (*12, 25-28*). Therapy-resistant LSCs are more reliant on oxidative
297 respiration than glycolysis for energy generation, suggesting that the OXPHOS dependency
298 and lack of normal glycolytic activity in LSCs may be characteristic of cancers (*29*).
299 Understanding resistance mechanisms will allow for the design of strategies to counteract drug
300 resistance or impede resistance from developing. In AMLs with aberrant expression of BCL-
301 2, venetoclax can reduce OXPHOS (*9*) and trigger cell death. However, venetoclax resistance
302 can occur in patients treated with the BCL-2 inhibitor and in some subtypes of AML patients
303 with poor prognoses (*30*).

304

305 Previous work has indicated that AML cells display increased mitochondrial biogenesis and
306 inhibition of mitochondrial translation can be used as a strategy for human AML (*18, 27*). In
307 our work, we target another process involved in mitochondrial gene expression, i.e.,
308 transcription. IMT treatment targets POLRMT, which has two main functions in mitochondria:
309 it transcribes mtDNA encoded genes and provides the primers required to initiate mtDNA

310 replication. Inhibition of POLRMT can thus deliver a double punch, both reducing mtDNA
311 copy number and inhibit OXPHOS biogenesis. As demonstrated here inhibition of POLRMT
312 can overcome venetoclax therapy resistance in AML. These observations are in line with recent
313 reports of the importance of mitochondrial function in leukemia cell survival (*31, 32*). By
314 developing a clinically relevant and well-tolerated approach to deliver IMTs in
315 immunodeficient mice transplanted with AML cells, we were able to reduce the tumor burden
316 in all (cell- and patient-derived) xenografted mice treated with a combination of IMT and
317 venetoclax. This demonstrates that reducing POLRMT activity results in successful targeting
318 of leukemic cells. Our *in vitro* investigations confirmed that the combination of IMT and
319 venetoclax is necessary to significantly decrease ATP levels and consequently induce
320 apoptosis. In addition, efficacy studies of AML PDX models showed that single compounds
321 are not sufficient to eradicate AML cells, but that the combination regimen reduced AML
322 tumor burden and prolonged survival in all treated mice. These data indicate the advantage of
323 both downregulating POLRMT activity in combination with increasing apoptosis and
324 highlights the importance of rational combination therapies (*33, 34*).
325
326 In summary, we have introduced a new therapeutic strategy to target therapy-resistant leukemia
327 with OXPHOS-dependent properties. Despite several limitations with the design of pre-clinical
328 cancer models and the intensity and duration of treatments, we demonstrate here that the
329 combined inhibition of BCL-2 and mitochondrial transcription can target therapy-resistant
330 AMLs. This combination treatment succeeds as IMT primes cell vulnerability to apoptosis
331 induction. Consequently, our findings may be of value for the future development of better
332 clinical strategies for the treatment of AML.
333
334

335 **Materials and Methods**

336 **Cell lines and culture conditions**

337 All cell lines (MV4-11, MOLM13, THP-1, KG-1, OCI-AML3, and OCI-AML2) were
338 purchased from DSMZ (Braunschweig, Germany) and cultured in RPMI-1640 (Sigma Aldrich)
339 supplemented with 10–20% heat inactivated fetal bovine serum (Gibco) and 1%
340 penicillin/streptomycin (Invitrogen). Cells were maintained in a humidified incubator at 37 °C
341 and 5% CO_2. RPMI-1640 without glucose was used for *in vitro* treatment experiments and
342 supplemented by physiological concentrations (5 mM) of glucose (D-Glucose, Sigma) or
343 galactose (D-galactose, Sigma).

344

345 **Generation of *in vivo* AML mouse model**

346 Mice were purchased from Jackson laboratories (USA) and maintained in a pathogen-free
347 facility at the University of Gothenburg. All animal experiments were conducted in accordance
348 with guidelines approved by the research animal ethics committee at the University of
349 Gothenburg. For AML cell line xenograft (CDX) experiments, 6–8-week-old, male NBSGW
350 mice (NOD.Cg-Kit^{W-41J} Tyr^{+} Prkdc^{scid} Il2rg^{tm1Wjl}/ThomJ, Jackson laboratories) were used.
351 Mice were transplanted intravenously with ~1 × 10^6 MV4-11 cells. For patient-derived
352 xenograft (PDX) experiments, 6–8-week-old, male NSGS mice (NOD.Cg-Prkdc^{scid} Il2rg^{tm1Wjl}
353 Tg(CMV-IL3,CSF2,KITLG)1Eav/MloySzJ, Jackson laboratories) were sub-lethally irradiated
354 with 1 Gy radiation. AML PDX splenocytes were purchased from Jackson laboratories (id:
355 J000106134*, Positive for FLT3-ITD, DNMT3A, and NPM1mutaions; and id: 000106566*,
356 Positive for TP53 mutation). Mice were transplanted intravenously with ~1 × 10^6 splenocytes
357 from AML PDX mice containing more than 80% patient AML cells.

358

359 **Human leukemia cell frequency assessment by flow cytometry**

360 The percentage of human leukemic cells (MV4-11 cell lines and AML PDX cells) in mouse
361 peripheral blood, BM, and spleen was determined by flow cytometry. Mice were bled at
362 indicated time points after transplantation. Prior to staining, peripheral red blood cells were
363 lyzed using ammonium chloride for 8–10 min at room temperature. Cells were stained with
364 antibodies, washed, and submitted for flow-cytometric analysis using a FACS Aria (BD
365 Biosciences, USA) or CytoFlex instrument (Beckman Coulter, California, USA). At least
366 10,000 events were acquired, and the percentage was calculated relative to gated viable
367 mononuclear cells (MNCs). To discriminate between human and mouse cells, cells were
368 stained with antibodies against human CD45 (clone HI30, BD Biosciences) and mouse CD45
369 (clone 2D1, BD Biosciences). Engraftment was deemed positive if human CD45+ cells
370 represented >0.1% of the viable MNCs. 7AAD (BD Biosciences) served as viability marker.
371

372 **Preparation of compounds for *in vivo* drug administration**

373 IMT was optimized based on the structure activity and property relationship of the coumarin
374 mtRNAPol inhibitor class by LDC (Dortmund, Germany). Venetoclax was obtained from
375 MedChemExpress (Hölzel Diagnostika Handels GmbH, Germany). Following the
376 development of a suitable vehicle for the formulation of IMT and venetoclax, as well as the
377 combination of both compounds, the test articles were formulated using 0.5% aqueous
378 methylcellulose solution (Sigma-Aldrich, Germany). After randomization, and two weeks
379 post-transplantation or with confirmation of engraftment, mice were treated with vehicle (0.5%
380 methylcellulose), 50 mg/kg IMT, 100 mg/kg venetoclax, or a combination (100 mg/kg
381 venetoclax + 50 mg/kg IMT) by oral administration daily for 21 days.
382

383 **Cell proliferation assay**

384 Cells were seeded out ca 20 h prior to treatment. For dose response experiments, cells were
385 treated with a wide range of concentrations of single compounds. Cell proliferation assays were
386 performed every 24 h from 72–168 h, where cell viability/ATP production was determined
387 using CellTiter-Glo (Promega).
388
389 **Apoptosis assay and Mitochondrial potential assay**
390 Apoptosis was evaluated by Annexin V and PI staining and mitochondrial membrane potential
391 was evaluated by lipophilic cationic dye JC-1. Cells were treated with IC50 concentrations of
392 IMT, venetoclax, or combination of both, analyzed using an advanced image cytometer
393 (Nucleocounter NucleoCounter's accompanying software NucleoView).
394
395 **High-resolution respirometry**
396 AML cell lines were treated with DMSO, IMT, venetoclax, or combination of IMT and
397 venetoclax for 3–4 days. The mitochondrial respiratory capacity (oxygen consumption rate)
398 was measured using high resolution respirometry (O2K, Oroboros, Innsbruck, Austria). A
399 substrate-uncoupler-inhibitor titration (SUIT) protocol was used to measure specific features
400 of mitochondrial respiration. Respiratory capacities were tested in a sequence of coupling
401 states: basal respiration; LEAK respiration using 5 mM oligomycin (Sigma); and non-coupled
402 electron transfer state (ET state) where the optimum carbonyl cyanide 3-
403 chlorophenylhydrazone (CCCP, Sigma) concentration for maximum flux was determined by
404 titration (max. 3 μM CCCP). Mitochondrial respiration was inhibited using 2.5 μM antimycin
405 (Sigma). Where stated, excess glucose (D-Glucose, Merck) was added at a final concentration
406 of 20 mM. Instrumental and oxygen background fluxes were calibrated as a function of oxygen
407 concentration and subtracted from the total volume-specific oxygen flux. Calibration and data
408 analysis was performed using Datlab v.6.1 software (Oroboros Instruments).

409

410 **Pharmacokinetics analysis**

411 IMT and venetoclax were extracted from plasma and tissues by protein precipitation using
412 acetonitrile. Tissue samples were homogenized using double the (sample) volume of PBS, and
413 bone marrow samples were suspended in 40 µL of PBS prior to extraction with acetonitrile.
414 Samples were analyzed by liquid chromatography tandem-mass spectrometry using a
415 Prominence UFLC system (Shimadzu) coupled to a Qtrap 5500 instrument (ABSciex). Test
416 articles were separated on a C18 column using a gradient elution with an acetonitrile/water
417 mixture containing 0.1% formic acid as the mobile phase. Chromatographic conditions and
418 mass spectrometry parameters were optimized for each test article prior to sample analysis.
419 Concentrations of each test article were calculated by means of a standard curve.

420

421 **mRNA extraction and transcriptome sequencing of AML PDX cells**

422 For RNAseq experiment BM samples were FACS sorted using BD FACS Aria fusion (BD
423 Biosciences). Human AML cells were isolated using human CD45 antibody. 7-AAD (BD
424 Biosciences) was used for dead cell exclusion. RNA was extracted using RNeasy Micro kit
425 (Qiagen). RNAseq library preparation and RNA-sequencing was done using the SMARTer
426 Total Stranded RNA pico kit. RNA library was prepared at National Genomics Infrastructure
427 (NGI) to be sequenced on the NovaSeq S6000 on 0.5 lanes of one S4 flowcell.

428

429 **Bioinformatics analysis**

430 Analysis was performed in R (www.r-project.org, accessed on 10 May 2022) using DESeq2,
431 clusterProfiler and ReactomePA packages. Prefiltering to keep genes that have at least 10 reads
432 total was performed before differential expression analysis was done with DESeq2.
433 Visualization of differentially expressed genes was done with EnhancedVolcano to create

434 volcano plots and gridExtra for creating tables. The *p*-value cutoff was set to 0.1 to allow for
435 more genes to be found in EP (End-of-treatment) group comparisons and the Res/Sen
436 (Resistant/Sensitive) group comparisons. Upregulated and downregulated genes were plotted
437 and colored according to Fold Change (FC) greater than 1.5 or -1.5 and the *p*-value cutoff 0.1.
438

439 **Statistical Analysis**

440 Unless otherwise noted, data were summarized using mean ± standard error of the mean (±
441 SEM). Per-group sample sizes presented in figures and results are reported from ≥3 separate
442 experiments, unless stated otherwise. Survival distributions were estimated using the Kaplan–
443 Meier method, and group comparisons were conducted using the log-rank test. Data were
444 analyzed using GraphPad Prism 9.0. Combination analysis was summarized using the Bliss-
445 independent model (*16*). The formula $Y_{ab,P} = Y_a + Y_b - Y_aY_b$ was used where drug A at dose a
446 inhibits Y_a percent of cell growth, and drug B at dose b inhibits Y_b percent of cell growth. The
447 predicted inhibitory effect of combined percentage was estimated by $Y_{ab,P}$. The observed
448 combined percentage inhibition $Y_{ab,O}$ was then compared with $Y_{ab,P}$, and if $Y_{ab,O} > Y_{ab,P}$, the
449 combination treatment was thought to be more efficacious (synergy). If $Y_{ab,O} = Y_{ab,P}$ the
450 combination treatment was thought to be additive.
451

452 **References**

453 1. R. Guieze, V. M. Liu, D. Rosebrock, A. A. Jourdain, M. Hernandez-Sanchez, A. Martinez
454 Zurita, J. Sun, E. Ten Hacken, K. Baranowski, P. A. Thompson, J. M. Heo, Z. Cartun, O.
455 Aygun, J. B. Iorgulescu, W. Zhang, G. Notarangelo, D. Livitz, S. Li, M. S. Davids, A. Biran,
456 S. M. Fernandes, J. R. Brown, A. Lako, Z. B. Ciantra, M. A. Lawlor, D. B. Keskin, N. D.
457 Udeshi, W. G. Wierda, K. J. Livak, A. G. Letai, D. Neuberg, J. W. Harper, S. A. Carr, F.
458 Piccioni, C. J. Ott, I. Leshchiner, C. M. Johannessen, J. Doench, V. K. Mootha, G. Getz, C. J.
459 Wu, Mitochondrial Reprogramming Underlies Resistance to BCL-2 Inhibition in Lymphoid
460 Malignancies. *Cancer Cell* **36**, 369-384 e313 (2019).

461 2. A. J. Souers, J. D. Leverson, E. R. Boghaert, S. L. Ackler, N. D. Catron, J. Chen, B. D.
462 Dayton, H. Ding, S. H. Enschede, W. J. Fairbrother, D. C. Huang, S. G. Hymowitz, S. Jin, S.
463 L. Khaw, P. J. Kovar, L. T. Lam, J. Lee, H. L. Maecker, K. C. Marsh, K. D. Mason, M. J.
464 Mitten, P. M. Nimmer, A. Oleksijew, C. H. Park, C. M. Park, D. C. Phillips, A. W. Roberts,
465 D. Sampath, J. F. Seymour, M. L. Smith, G. M. Sullivan, S. K. Tahir, C. Tse, M. D. Wendt,
466 Y. Xiao, J. C. Xue, H. Zhang, R. A. Humerickhouse, S. H. Rosenberg, S. W. Elmore, ABT-
467 199, a potent and selective BCL-2 inhibitor, achieves antitumor activity while sparing
468 platelets. *Nat Med* **19**, 202-208 (2013).

469 3. M. Konopleva, D. A. Pollyea, J. Potluri, B. Chyla, L. Hogdal, T. Busman, E. McKeegan, A.
470 H. Salem, M. Zhu, J. L. Ricker, W. Blum, C. D. DiNardo, T. Kadia, M. Dunbar, R. Kirby, N.
471 Falotico, J. Leverson, R. Humerickhouse, M. Mabry, R. Stone, H. Kantarjian, A. Letai,
472 Efficacy and Biological Correlates of Response in a Phase II Study of Venetoclax
473 Monotherapy in Patients with Acute Myelogenous Leukemia. *Cancer Discov* **6**, 1106-1117
474 (2016).

475 4. A. W. Roberts, A. H. Wei, D. C. S. Huang, BCL2 and MCL1 inhibitors for hematologic
476 malignancies. *Blood* **138**, 1120-1136 (2021).

477 5. H. E. Ramsey, M. A. Fischer, T. Lee, A. E. Gorska, M. P. Arrate, L. Fuller, K. L. Boyd, S. A.
478 Strickland, J. Sensintaffar, L. J. Hogdal, G. D. Ayers, E. T. Olejniczak, S. W. Fesik, M. R.
479 Savona, A Novel MCL1 Inhibitor Combined with Venetoclax Rescues Venetoclax-Resistant
480 Acute Myelogenous Leukemia. *Cancer Discov* **8**, 1566-1581 (2018).

481 6. J. H. Choi, J. M. Bogenberger, R. Tibes, Targeting Apoptosis in Acute Myeloid Leukemia:
482 Current Status and Future Directions of BCL-2 Inhibition with Venetoclax and Beyond.
483 *Target Oncol* **15**, 147-162 (2020).

484 7. T. Nechiporuk, S. E. Kurtz, O. Nikolova, T. Liu, C. L. Jones, A. D'Alessandro, R. Culp-Hill,
485 A. d'Almeida, S. K. Joshi, M. Rosenberg, C. E. Tognon, A. V. Danilov, B. J. Druker, B. H.
486 Chang, S. K. McWeeney, J. W. Tyner, The TP53 Apoptotic Network Is a Primary Mediator
487 of Resistance to BCL2 Inhibition in AML Cells. *Cancer Discov* **9**, 910-925 (2019).

488 8. R. Pan, V. Ruvolo, H. Mu, J. D. Leverson, G. Nichols, J. C. Reed, M. Konopleva, M.
489 Andreeff, Synthetic Lethality of Combined Bcl-2 Inhibition and p53 Activation in AML:
490 Mechanisms and Superior Antileukemic Efficacy. *Cancer Cell* **32**, 748-760 e746 (2017).

491 9. E. D. Lagadinou, A. Sach, K. Callahan, R. M. Rossi, S. J. Neering, M. Minhajuddin, J. M.
492 Ashton, S. Pei, V. Grose, K. M. O'Dwyer, J. L. Liesveld, P. S. Brookes, M. W. Becker, C. T.
493 Jordan, BCL-2 inhibition targets oxidative phosphorylation and selectively eradicates
494 quiescent human leukemia stem cells. *Cell Stem Cell* **12**, 329-341 (2013).

495 10. T. Farge, E. Saland, F. de Toni, N. Aroua, M. Hosseini, R. Perry, C. Bosc, M. Sugita, L.
496 Stuani, M. Fraisse, S. Scotland, C. Larrue, H. Boutzen, V. Feliu, M. L. Nicolau-Travers, S.
497 Cassant-Sourdy, N. Broin, M. David, N. Serhan, A. Sarry, S. Tavitian, T. Kaoma, L. Vallar, J.
498 Iacovoni, L. K. Linares, C. Montersino, R. Castellano, E. Griessinger, Y. Collette, O.
499 Duchamp, Y. Barreira, P. Hirsch, T. Palama, L. Gales, F. Delhommeau, B. H. Garmy-Susini,
500 J. C. Portais, F. Vergez, M. Selak, G. Danet-Desnoyers, M. Carroll, C. Recher, J. E. Sarry,

501 Chemotherapy-Resistant Human Acute Myeloid Leukemia Cells Are Not Enriched for
502 Leukemic Stem Cells but Require Oxidative Metabolism. *Cancer Discov* **7**, 716-735 (2017).

503 11. E. M. Kuntz, P. Baquero, A. M. Michie, K. Dunn, S. Tardito, T. L. Holyoake, G. V.
504 Helgason, E. Gottlieb, Targeting mitochondrial oxidative phosphorylation eradicates therapy-
505 resistant chronic myeloid leukemia stem cells. *Nat Med* **23**, 1234-1240 (2017).

506 12. C. L. Jones, B. M. Stevens, A. D'Alessandro, J. A. Reisz, R. Culp-Hill, T. Nemkov, S. Pei, N.
507 Khan, B. Adane, H. Ye, A. Krug, D. Reinhold, C. Smith, J. DeGregori, D. A. Pollyea, C. T.
508 Jordan, Inhibition of Amino Acid Metabolism Selectively Targets Human Leukemia Stem
509 Cells. *Cancer Cell* **34**, 724-740 e724 (2018).

510 13. K. Henkenius, B. H. Greene, C. Barckhausen, R. Hartmann, M. Marken, T. Kaiser, M.
511 Rehberger, S. K. Metzelder, W. J. Parak, A. Neubauer, C. Brendel, E. Mack, Maintenance of
512 cellular respiration indicates drug resistance in acute myeloid leukemia. *Leuk Res* **62**, 56-63
513 (2017).

514 14. N. A. Bonekamp, B. Peter, H. S. Hillen, A. Felser, T. Bergbrede, A. Choidas, M. Horn, A.
515 Unger, R. Di Lucrezia, I. Atanassov, X. Li, U. Koch, S. Menninger, J. Boros, P. Habenberger,
516 P. Giavalisco, P. Cramer, M. S. Denzel, P. Nussbaumer, B. Klebl, M. Falkenberg, C. M.
517 Gustafsson, N. G. Larsson, Small-molecule inhibitors of human mitochondrial DNA
518 transcription. *Nature* **588**, 712-716 (2020).

519 15. B. A. Jonas, D. A. Pollyea, How we use venetoclax with hypomethylating agents for the
520 treatment of newly diagnosed patients with acute myeloid leukemia. *Leukemia* **33**, 2795-2804
521 (2019).

522 16. W. Zhao, K. Sachsenmeier, L. Zhang, E. Sult, R. E. Hollingsworth, H. Yang, A New Bliss
523 Independence Model to Analyze Drug Combination Data. *J Biomol Screen* **19**, 817-821
524 (2014).

525 17. N. Chapuis, L. Poulain, R. Birsen, J. Tamburini, D. Bouscary, Rationale for Targeting
526 Deregulated Metabolic Pathways as a Therapeutic Strategy in Acute Myeloid Leukemia.
527 *Front Oncol* **9**, 405 (2019).

528 18. D. Sharon, S. Cathelin, S. Mirali, J. M. Di Trani, D. J. Yanofsky, K. A. Keon, J. L.
529 Rubinstein, A. D. Schimmer, T. Ketela, S. M. Chan, Inhibition of mitochondrial translation
530 overcomes venetoclax resistance in AML through activation of the integrated stress response.
531 *Sci Transl Med* **11**, (2019).

532 19. B. L. Ebert, J. Pretz, J. Bosco, C. Y. Chang, P. Tamayo, N. Galili, A. Raza, D. E. Root, E.
533 Attar, S. R. Ellis, T. R. Golub, Identification of RPS14 as a 5q- syndrome gene by RNA
534 interference screen. *Nature* **451**, 335-339 (2008).

535 20. J. P. Patel, M. Gonen, M. E. Figueroa, H. Fernandez, Z. Sun, J. Racevskis, P. Van
536 Vlierberghe, I. Dolgalev, S. Thomas, O. Aminova, K. Huberman, J. Cheng, A. Viale, N. D.
537 Socci, A. Heguy, A. Cherry, G. Vance, R. R. Higgins, R. P. Ketterling, R. E. Gallagher, M.
538 Litzow, M. R. van den Brink, H. M. Lazarus, J. M. Rowe, S. Luger, A. Ferrando, E. Paietta,
539 M. S. Tallman, A. Melnick, O. Abdel-Wahab, R. L. Levine, Prognostic relevance of
540 integrated genetic profiling in acute myeloid leukemia. *N Engl J Med* **366**, 1079-1089 (2012).

541 21. U. Testa, Leukemia stem cells. *Ann Hematol* **90**, 245-271 (2011).

542 22. M. R. Savona, J. C. Rathmell, Mitochondrial Homeostasis in AML and Gasping for Response
543 in Resistance to BCL2 Blockade. *Cancer Discov* **9**, 831-833 (2019).

544 23. K. H. Lin, P. S. Winter, A. Xie, C. Roth, C. A. Martz, E. M. Stein, G. R. Anderson, J. P.
545 Tingley, K. C. Wood, Targeting MCL-1/BCL-XL Forestalls the Acquisition of Resistance to
546 ABT-199 in Acute Myeloid Leukemia. *Sci Rep* **6**, 27696 (2016).

547 24. N. P. Basak, S. Banerjee, Mitochondrial dependency in progression of acute myeloid
548 leukemia. *Mitochondrion* **21**, 41-48 (2015).

549 25. D. A. Pollyea, B. M. Stevens, C. L. Jones, A. Winters, S. Pei, M. Minhajuddin, A.
550 D'Alessandro, R. Culp-Hill, K. A. Riemondy, A. E. Gillen, J. R. Hesselberth, D. Abbott, D.
551 Schatz, J. A. Gutman, E. Purev, C. Smith, C. T. Jordan, Venetoclax with azacitidine disrupts
552 energy metabolism and targets leukemia stem cells in patients with acute myeloid leukemia.
553 *Nat Med* **24**, 1859-1866 (2018).

554 26. A. Cole, Z. Wang, E. Coyaud, V. Voisin, M. Gronda, Y. Jitkova, R. Mattson, R. Hurren, S.
555 Babovic, N. Maclean, I. Restall, X. Wang, D. V. Jeyaraju, M. A. Sukhai, S. Prabha, S. Bashir,
556 A. Ramakrishnan, E. Leung, Y. H. Qia, N. Zhang, K. R. Combes, T. Ketela, F. Lin, W. A.
557 Houry, A. Aman, R. Al-Awar, W. Zheng, E. Wienholds, C. J. Xu, J. Dick, J. C. Wang, J.
558 Moffat, M. D. Minden, C. J. Eaves, G. D. Bader, Z. Hao, S. M. Kornblau, B. Raught, A. D.
559 Schimmer, Inhibition of the Mitochondrial Protease ClpP as a Therapeutic Strategy for
560 Human Acute Myeloid Leukemia. *Cancer Cell* **27**, 864-876 (2015).

561 27. M. Skrtic, S. Sriskanthadevan, B. Jhas, M. Gebbia, X. Wang, Z. Wang, R. Hurren, Y. Jitkova,
562 M. Gronda, N. Maclean, C. K. Lai, Y. Eberhard, J. Bartoszko, P. Spagnuolo, A. C. Rutledge,
563 A. Datti, T. Ketela, J. Moffat, B. H. Robinson, J. H. Cameron, J. Wrana, C. J. Eaves, M. D.
564 Minden, J. C. Wang, J. E. Dick, K. Humphries, C. Nislow, G. Giaever, A. D. Schimmer,
565 Inhibition of mitochondrial translation as a therapeutic strategy for human acute myeloid
566 leukemia. *Cancer Cell* **20**, 674-688 (2011).

567 28. J. R. Molina, Y. Sun, M. Protopopova, S. Gera, M. Bandi, C. Bristow, T. McAfoos, P.
568 Morlacchi, J. Ackroyd, A. A. Agip, G. Al-Atrash, J. Asara, J. Bardenhagen, C. C. Carrillo, C.
569 Carroll, E. Chang, S. Ciurea, J. B. Cross, B. Czako, A. Deem, N. Daver, J. F. de Groot, J. W.
570 Dong, N. Feng, G. Gao, J. Gay, M. G. Do, J. Greer, V. Giuliani, J. Han, L. Han, V. K. Henry,
571 J. Hirst, S. Huang, Y. Jiang, Z. Kang, T. Khor, S. Konoplev, Y. H. Lin, G. Liu, A. Lodi, T.
572 Lofton, H. Ma, M. Mahendra, P. Matre, R. Mullinax, M. Peoples, A. Petrocchi, J. Rodriguez-
573 Canale, R. Serreli, T. Shi, M. Smith, Y. Tabe, J. Theroff, S. Tiziani, Q. Xu, Q. Zhang, F.
574 Muller, R. A. DePinho, C. Toniatti, G. F. Draetta, T. P. Heffernan, M. Konopleva, P. Jones,
575 M. E. Di Francesco, J. R. Marszalek, An inhibitor of oxidative phosphorylation exploits
576 cancer vulnerability. *Nat Med* **24**, 1036-1046 (2018).

577 29. J. Kreitz, C. Schonfeld, M. Seibert, V. Stolp, I. Alshamleh, T. Oellerich, B. Steffen, H.
578 Schwalbe, F. Schnutgen, N. Kurrle, H. Serve, Metabolic Plasticity of Acute Myeloid
579 Leukemia. *Cells* **8**, (2019).

580 30. A. N. Saliba, A. J. John, S. H. Kaufmann, Resistance to venetoclax and hypomethylating
581 agents in acute myeloid leukemia. *Cancer Drug Resist* **4**, 125-142 (2021).

582 31. I. Baccelli, Y. Gareau, B. Lehnertz, S. Gingras, J. F. Spinella, S. Corneau, N. Mayotte, S.
583 Girard, M. Frechette, V. Blouin-Chagnon, K. Leveille, I. Boivin, T. MacRae, J. Krosl, C.
584 Thiollier, V. P. Lavallee, E. Kanshin, T. Bertomeu, J. Coulombe-Huntington, C. St-Denis, M.
585 E. Bordeleau, G. Boucher, P. P. Roux, S. Lemieux, M. Tyers, P. Thibault, J. Hebert, A.
586 Marinier, G. Sauvageau, Mubritinib Targets the Electron Transport Chain Complex I and
587 Reveals the Landscape of OXPHOS Dependency in Acute Myeloid Leukemia. *Cancer Cell*
588 **36**, 84-99 e88 (2019).

589 32. C. Bosc, M. A. Selak, J. E. Sarry, Resistance Is Futile: Targeting Mitochondrial Energetics
590 and Metabolism to Overcome Drug Resistance in Cancer Treatment. *Cell Metab* **26**, 705-707
591 (2017).

592 33. M. Hosseini, H. R. Rezvani, N. Aroua, C. Bosc, T. Farge, E. Saland, V. Guyonnet-Duperat, S.
593 Zaghdoudi, L. Jarrou, C. Larrue, M. Sabatier, P. L. Mouchel, M. Gotanegre, M. Piechaczyk,
594 G. Bossis, C. Recher, J. E. Sarry, Targeting Myeloperoxidase Disrupts Mitochondrial Redox
595 Balance and Overcomes Cytarabine Resistance in Human Acute Myeloid Leukemia. *Cancer*
596 *Res* **79**, 5191-5203 (2019).

34. S. Jin, D. Cojocari, J. J. Purkal, R. Popovic, N. N. Talaty, Y. Xiao, L. R. Solomon, E. R. Boghaert, J. D. Leverson, D. C. Phillips, 5-Azacitidine Induces NOXA to Prime AML Cells for Venetoclax-Mediated Apoptosis. *Clin Cancer Res* **26**, 3371-3383 (2020).

603 **Acknowledgments**

604 **General:**

605 The authors would like to thank the staff at the Department of Experimental Biomedicine at
606 the University of Gothenburg, namely, Jenny Nyman, Claudia Engwall, Tova Johansson and
607 Hanna Brissman for tremendous assistance with mouse experiments. They would also like to
608 thank Dr Rebekah Hailes for editing the manuscript and to acknowledge Lenka Palova-
609 Jelinkova, Klara Danova, and Pavla Jestrabova from SOTIO Biotech (Prague, Czech Republic)
610 for valuable input on *in vitro* and *in vivo* studies. The authors acknowledge support from the
611 National Genomics Infrastructure in Stockholm funded by Science for Life Laboratory, the
612 Knut and Alice Wallenberg Foundation and the Swedish Research Council, and SNIC/Uppsala
613 Multidisciplinary Center for Advanced Computational Science for assistance with massively
614 parallel sequencing and access to the UPPMAX computational infrastructure.

615

616 **Funding:**

617 Swedish Research Council grant 2017-01257 (CMG)

618 Swedish Cancer Foundation grant 20 1291 PjF (CMG)

619 Swedish Cancer Foundation grant 20 0925 PjF (LP)

620 Knut and Alice Wallenberg Foundation grant 2017.0080 (CMG)

621 The Swedish state under the agreement between the Swedish government and the county
622 councils, the ALF agreement grant ALFGBG-966275 (CMG)

623 The Swedish state under the agreement between the Swedish government and the county
624 councils, the ALF agreement grant ALFGBG-965206 (LP)

625 Assar Gabrielsson Foundation for cancer research grant (LSA)

626

627 **Author contributions:**

Conceptualization (LSA, RD, TB, AU, PN, BMK)

Methodology (TB, AU, PN, BMK)

Investigation (LSA, JA, CN)

Supervision (BMK, LP, CG)

Writing—original draft (LSA)

Writing—review & editing (LSA, JA, AU, RD, TB, PN, BMK, LP, CMG)

Competing interests:

CMG is a scientific co-founder of Pretzel Therapeutics Inc. Together with RD, TB, AU, PN, BMK who are employees of LDC, CMG is also co-inventor of the patent application WO 2019/057821. Medicinal chemistry and pharmacology part of this work was financed by the Max-Planck Gesellschaft e.V. under the framework agreement between Max-Planck and LDC.

Data and materials availability:

All data needed to evaluate the conclusions in the paper are present in the paper and/or the Supplementary Materials. RNA-seq datasets have been deposited in the GSE repository (GSE213976). Additional data related to this paper may be requested from the authors.

Figure 1

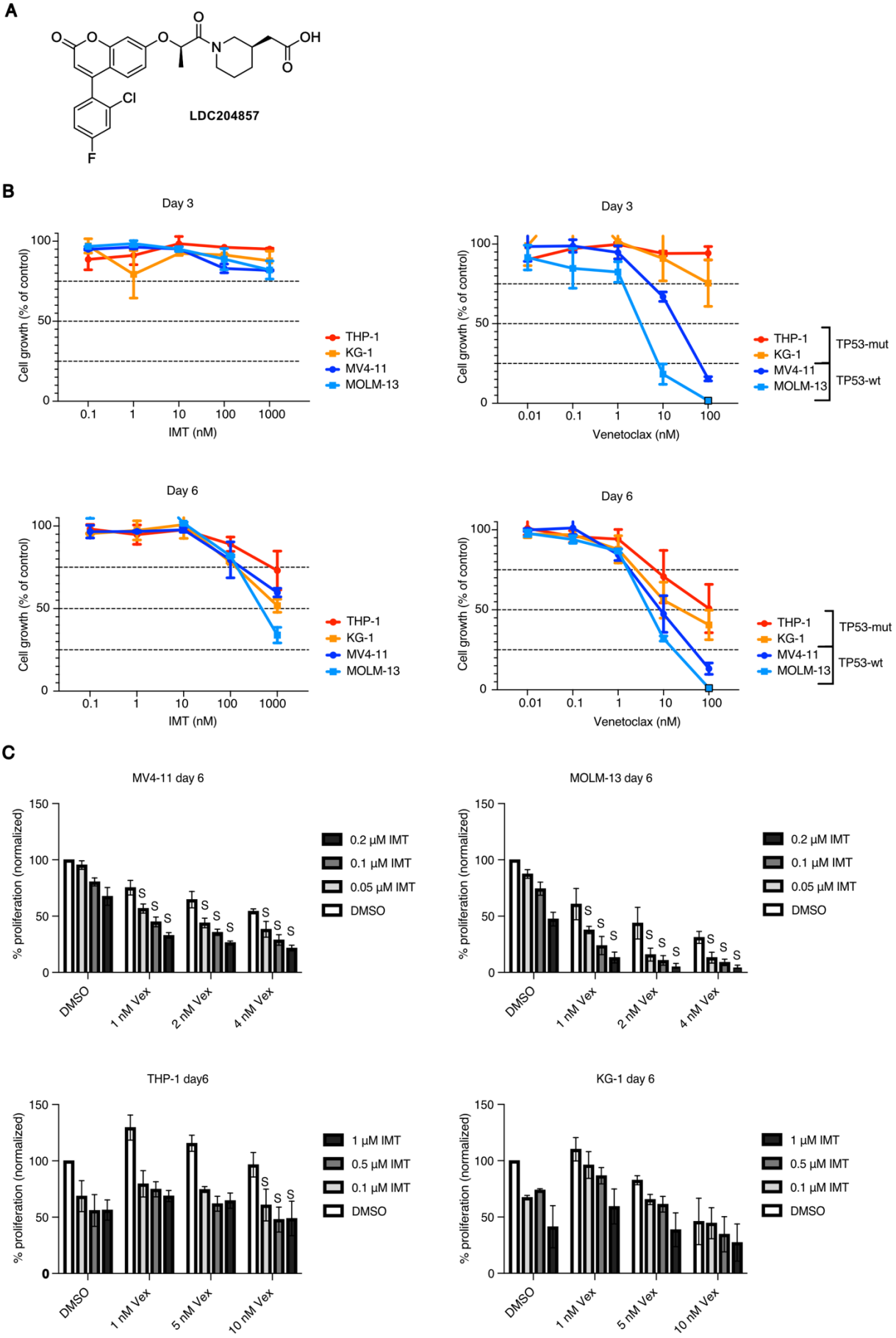
A
LDC204857
B
Day 3
Cell growth (% of control)
IMT (nM)
THP-1
KG-1
MV4-11
MOLM-13
Venetoclax (nM)
TP53-mut
TP53-wt
Day 6
C
MV4-11 day 6
MOLM-13 day 6
THP-1 day6
KG-1 day 6
% proliferation (normalized)
0.2 µM IMT
0.1 µM IMT
0.05 µM IMT
1 µM IMT
0.5 µM IMT
DMSO
1 nM Vex
2 nM Vex
4 nM Vex
5 nM Vex
10 nM Vex

648 **Figure 1. IMT+venetoclax combination treatment synergistically inhibits cell**
649 **viability/growth of AML cell lines *in vitro*.**
650 (**A**) Chemical structure of IMT (LDC204857) (**B**) AML cell lines were treated with single
651 agents IMT or venetoclax at a range of concentrations (0.1–1000 nM and 0.01–100 nM,
652 respectively), and assessed by cell viability tests after three and six days. (**C**) Synergism
653 analysis of AML cell lines treated with a combination of IMT (0.05, 0.1, 0.2 μM for MV4-11
654 and MOLM-13, and 0.1, 0.5, and 1 μM for THP-1 and KG-1) and venetoclax (Vex; 1, 2, 4 nM
655 for MV4-11 and MOLM-13, and 1, 5, 10 nM for THP-1 and KG-1) for six days. 'S' represents
656 synergy of the combination treatment, evaluated using the Bliss independent model.
657 Proliferation percentages are normalized to DMSO treated. All results are from three
658 independent experiments.
659

Figure 2

A

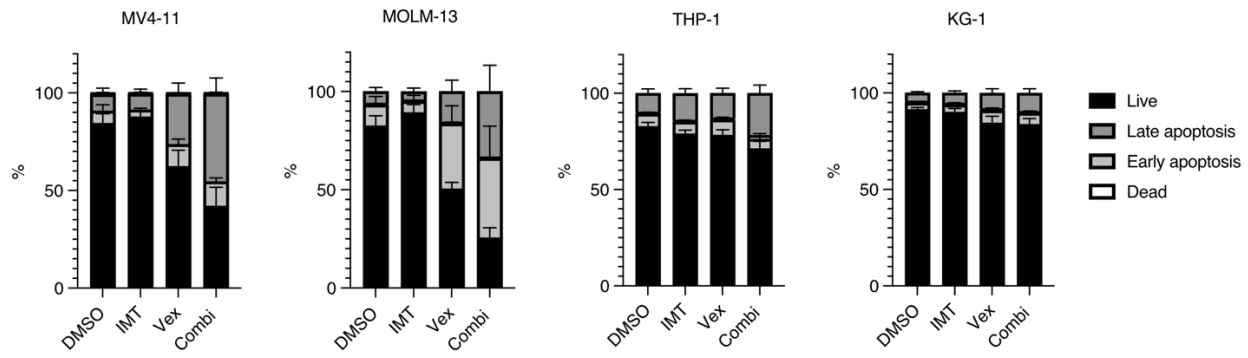

B

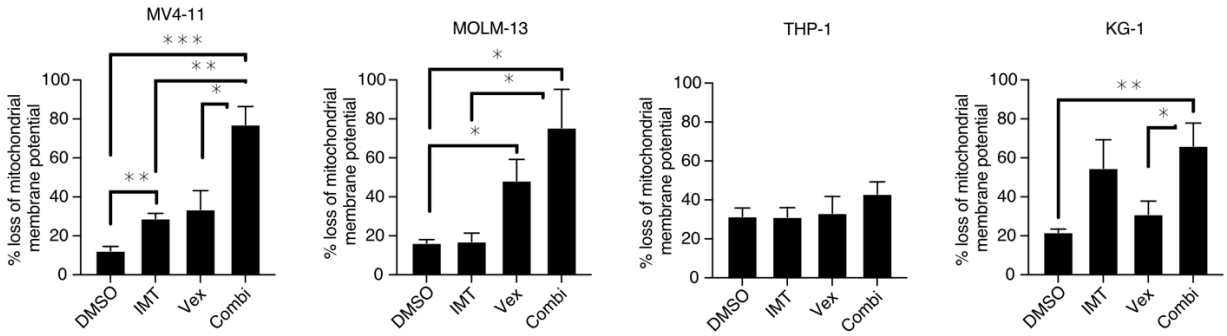

660

661 **Figure 2. Combination treatment significantly enhances apoptosis induction in AML cell**
662 **lines**.
663 AML cell lines were treated with IMT (500 nM) and venetoclax (5 nM) for 72–96 h. (**A**)
664 Apoptosis was determined by Annexin V/PI staining of the cells and analyzed by flow
665 cytometry. (**B**) Loss of mitochondrial membrane potential was calculated as the percentage of
666 depolarized (apoptotic) cells out of the total cell population. Error bars represent standard error
667 of the mean where * represents $P < 0.05$, **$P < 0.01$, and ***$p < 0.001$.
668

Figure 3

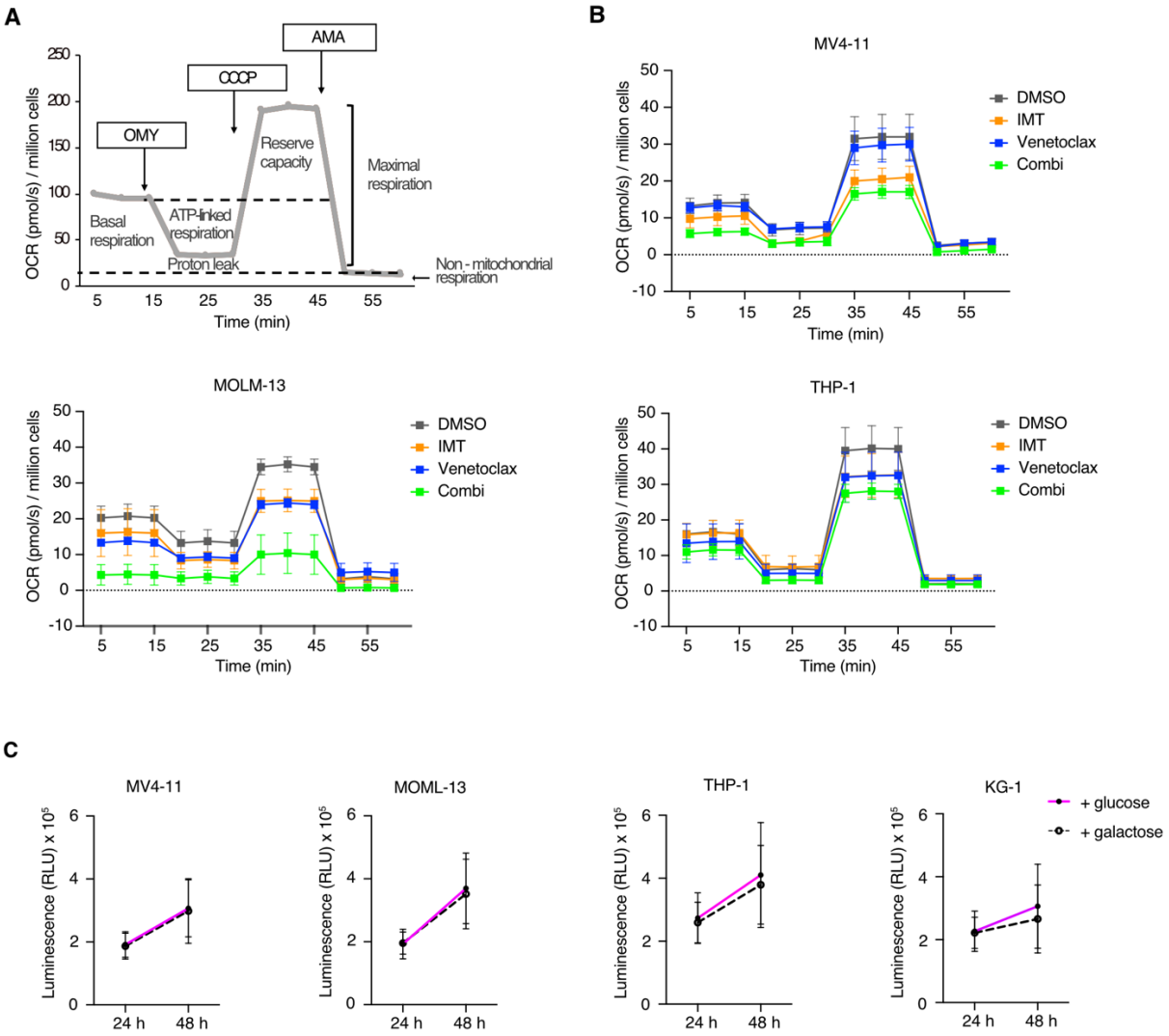
A
AMA
CCCP
OMY
Reserve capacity
Maximal respiration
Basal respiration
ATP-linked respiration
Proton leak
Non - mitochondrial respiration
OCR (pmol/s) / million cells
Time (min)
B
MV4-11
MOLM-13
THP-1
DMSO
IMT
Venetoclax
Combi
C
MV4-11
MOML-13
THP-1
KG-1
Luminescence (RLU) x 10^5
24 h
48 h
+ glucose
+ galactose

669

670 **Figure 3. Combination of IMT and venetoclax dramatically decreases OXPHOS (in a**
671 **glycolysis-independent manner) in sensitive cell lines.**
672 (**A**) Representative graph of an OXPHOS measurement using mitostress compounds:
673 oligomycin (OMY), carbonyl cyanide m-chlorophenyl hydrazone (CCCP), and antimycin
674 (AMA). (**B**) AML cell lines (MV4-11, MOLM-13, and THP-1) were treated with either IMT
675 (500 nM), venetoclax (5 nM), or a combination of both for four days. DMSO was added to
676 control wells. Oxygen consumption rate (OCR) was measured with an Oroboros O2K
677 instrument at physiological glucose levels (5 mM) using mitostress compounds. (**C**) AML cell
678 lines were cultured in growth medium supplemented with either 5 mM glucose or galactose,
679 and cell viability tests (ATP measurements) were performed after 24 and 48 h. All results are
680 from at least three independent experiments. Error bars show ± SEM. Statistical tests on all
681 comparisons in (C) showed non-significant differences.
682

Figure 4

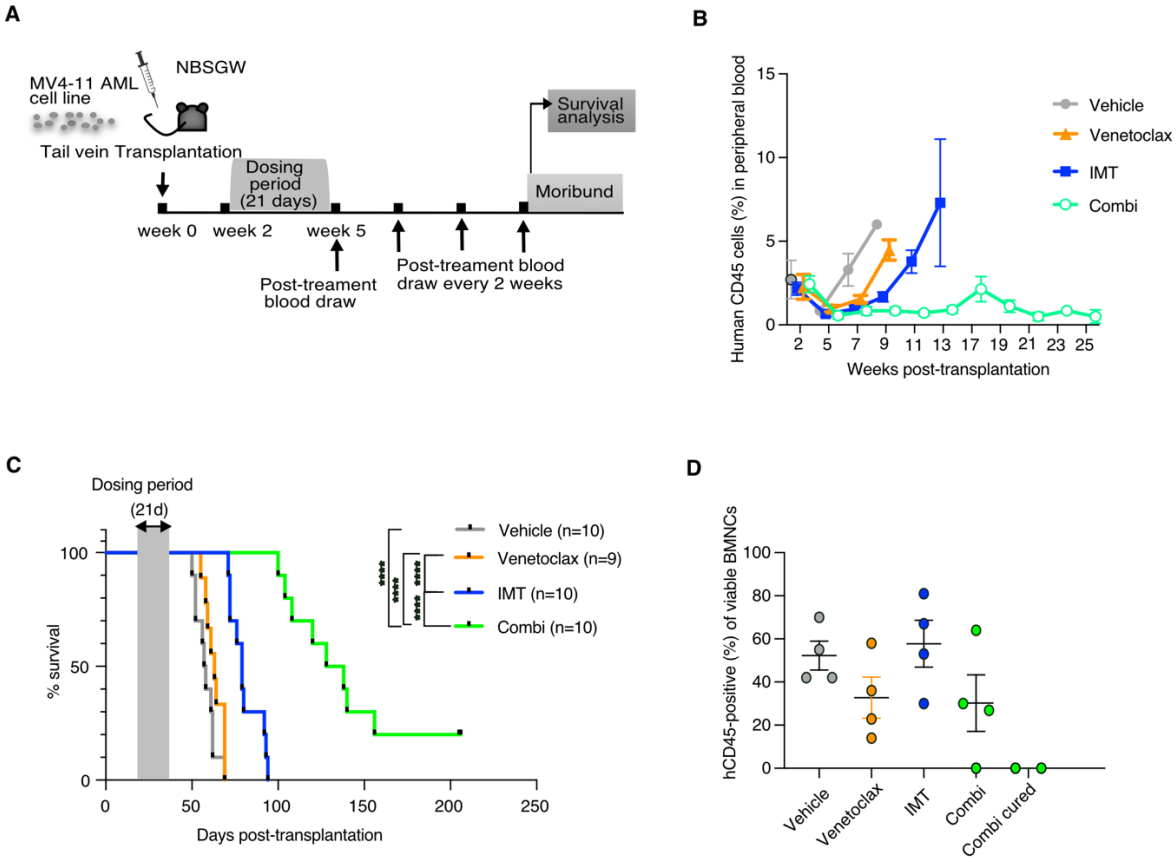
A
MV4-11 AML cell line
NBSGW
Tail vein Transplantation
Dosing period (21 days)
Survival analysis
Moribund
week 0
week 2
week 5
Post-treament blood draw
Post-treament blood draw every 2 weeks
B
Human CD45 cells (%) in peripheral blood
Weeks post-transplantation
Vehicle
Venetoclax
IMT
Combi
C
Dosing period (21d)
% survival
Days post-transplantation
Vehicle (n=10)
Venetoclax (n=9)
IMT (n=10)
Combi (n=10)
D
hCD45-positive (%) of viable BMNCs
Vehicle
Venetoclax
IMT
Combi
Combi cured

683

684 **Figure 4. Combination of IMT and venetoclax significantly prolongs the survival of mice**
685 **with leukemia.**
686 (**A**) Outline of CDX efficacy experiment: NBSGW mice were transplanted with MV4-11
687 human leukemia cells, then treated with either vehicle, IMT, venetoclax, or a combination of
688 IMT and venetoclax (n=10 per treatment group). Peripheral blood was taken before treatment
689 (week 2) and after treatment at regular intervals until disease progression was observed. (**B**)
690 Analysis of proportion of human CD45+ cells in mice peripheral blood in all treatment groups
691 at indicated time points, determined by flow cytometry. (**C**) Kaplan-Meier analysis of survival.
692 Statistical significance was calculated using log-rank (Mantle-Cox) test. ****$p < 0.0001$, Error
693 bars represent ± SEM. (**D**) Analysis of proportion of human CD45+ cells in the bone marrow
694 of all treatment groups at time of euthanization.
695
696

Figure 5

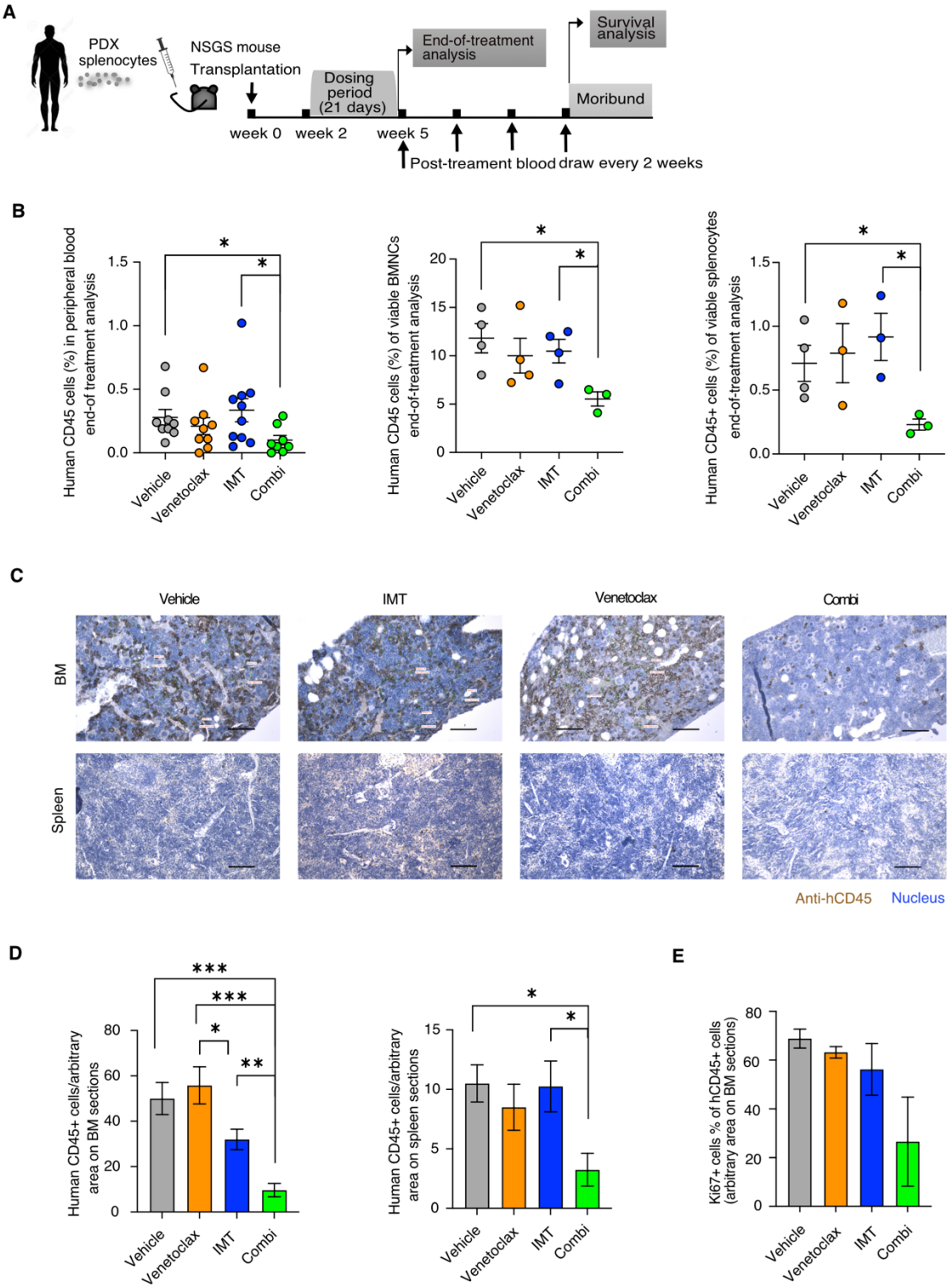
A
PDX splenocytes
NSGS mouse Transplantation
Dosing period (21 days)
End-of-treatment analysis
Survival analysis
Moribund
week 0
week 2
week 5
Post-treament blood draw every 2 weeks
B
Human CD45 cells (%) in peripheral blood end-of treatment analysis
Human CD45 cells (%) of viable BMNCs end-of-treatment analysis
Human CD45+ cells (%) of viable splenocytes end-of-treatment analysis
Vehicle
Venetoclax
IMT
Combi
C
Vehicle
IMT
Venetoclax
Combi
BM
Spleen
Anti-hCD45
Nucleus
D
Human CD45+ cells/arbitrary area on BM sections
Human CD45+ cells/arbitrary area on spleen sections
E
Ki67+ cells % of hCD45+ cells (arbitrary area on BM sections)

697

698 **Figure 5. Synergistic effect of (IMT and venetoclax) combination treatment on tumor**
699 **burden and survival of AML-PDX transplanted mice.**
700 (**A**) Experimental outline: NSGS mice were transplanted with primary AML splenocytes from
701 PDX mice and were then treated with either vehicle, IMT, venetoclax, or a combination of IMT
702 and venetoclax (n=10 per treatment group). After the final dosing, three or four mice were
703 euthanized (end-of-treatment group) and the rest (n=6) were maintained for survival analysis.
704 (**B**) Percentage of viable human CD45-positive (hCD45+) cells in peripheral blood, BM, and
705 spleen of treated mice determined by flow cytometry. (**C**) Immunohistochemistry analysis of
706 mouse BM and spleen sections stained with anti-human CD45 (brown) and counterstained with
707 DAB (blue). (**D**) Quantitative analysis of hCD45+ cells on immunohistochemistry sections of
708 BM and spleen sections of treated mice. (**E**) Proliferating tumor cells (CD45) are shown by
709 quantification of Ki67 positive cells in immunohistochemistry-stained BM sections at end-of-
710 treatment (results from at least three technical replicates and two biological replicates in each
711 treatment group).
712
713

Figure 6

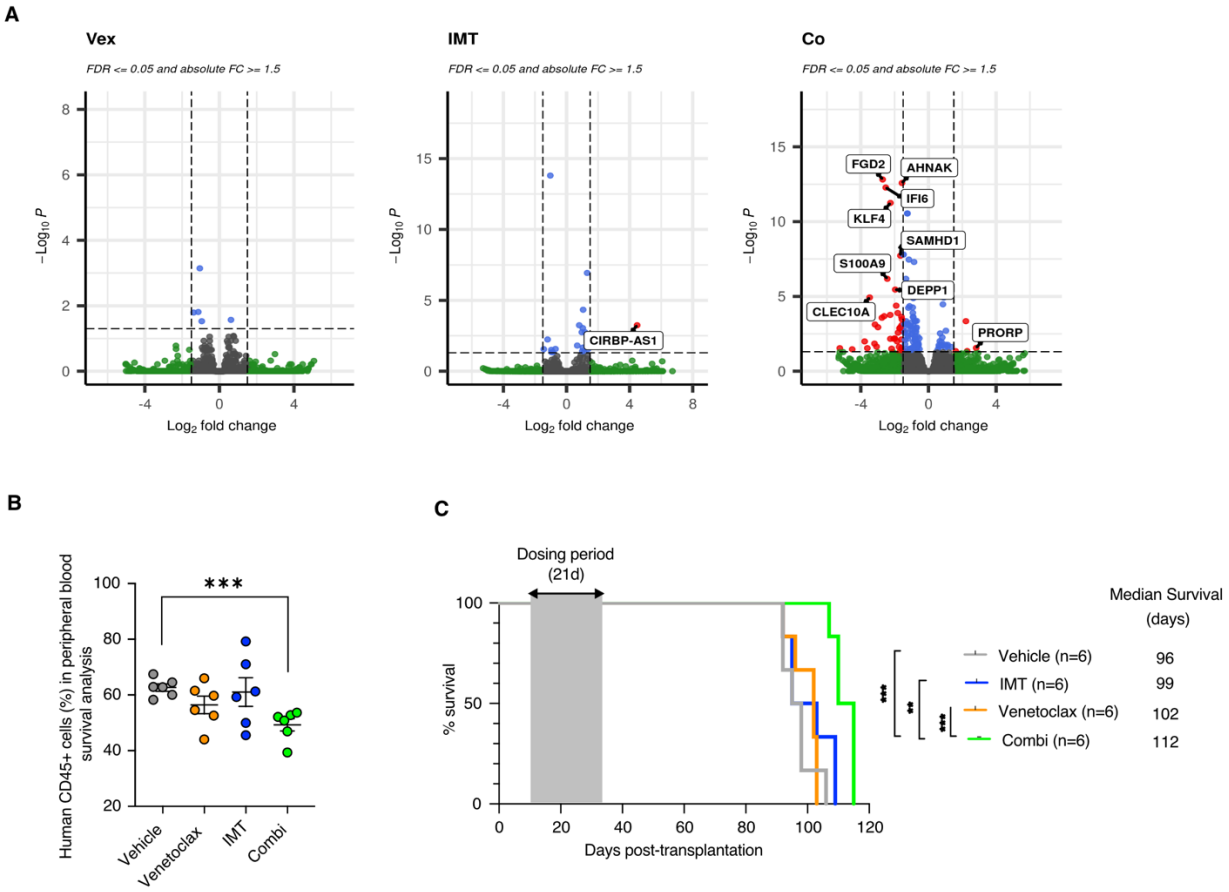
A
Vex
FDR <= 0.05 and absolute FC >= 1.5
IMT
FDR <= 0.05 and absolute FC >= 1.5
Co
FDR <= 0.05 and absolute FC >= 1.5
FGD2
AHNAK
IFI6
KLF4
SAMHD1
S100A9
DEPP1
CLEC10A
PRORP
CIRBP-AS1
−Log10 P
Log2 fold change
B
Human CD45+ cells (%) in peripheral blood survival analysis
***
Vehicle
Venetoclax
IMT
Combi
C
Dosing period (21d)
% survival
Days post-transplantation
Median Survival (days)
Vehicle (n=6) 96
IMT (n=6) 99
Venetoclax (n=6) 102
Combi (n=6) 112

714

715 **Figure 6. Synergistic effect of (IMT and venetoclax) combination treatment on gene**
716 **transcription and survival of AML-PDX transplanted mice.**
717 The experimental outline was shown in figure 5A, but n=10 per treatment group. After the final
718 dosing, three or four mice were euthanized (end-of-treatment group) and the rest (n=6) were
719 maintained for survival analysis. (**A**) Gene expression profiling by RNA-seq of purified AML
720 blasts isolated from PDX models treated with venetoclax, IMT, or a combination thereof.
721 Indicated expression changes are relative to a vehicle treated group. Significantly enriched
722 genes are indicated in red ($q < 0.05$). (**B**) Peripheral blood engraftment analysis of survival
723 group. (**C**) Survival analysis of treated mice shown by Kaplan-Meier analysis (n=6/treatment
724 group). *$P < 0.05$, **$P < 0.01$, and ***$p < 0.001$.
725

Figure 7

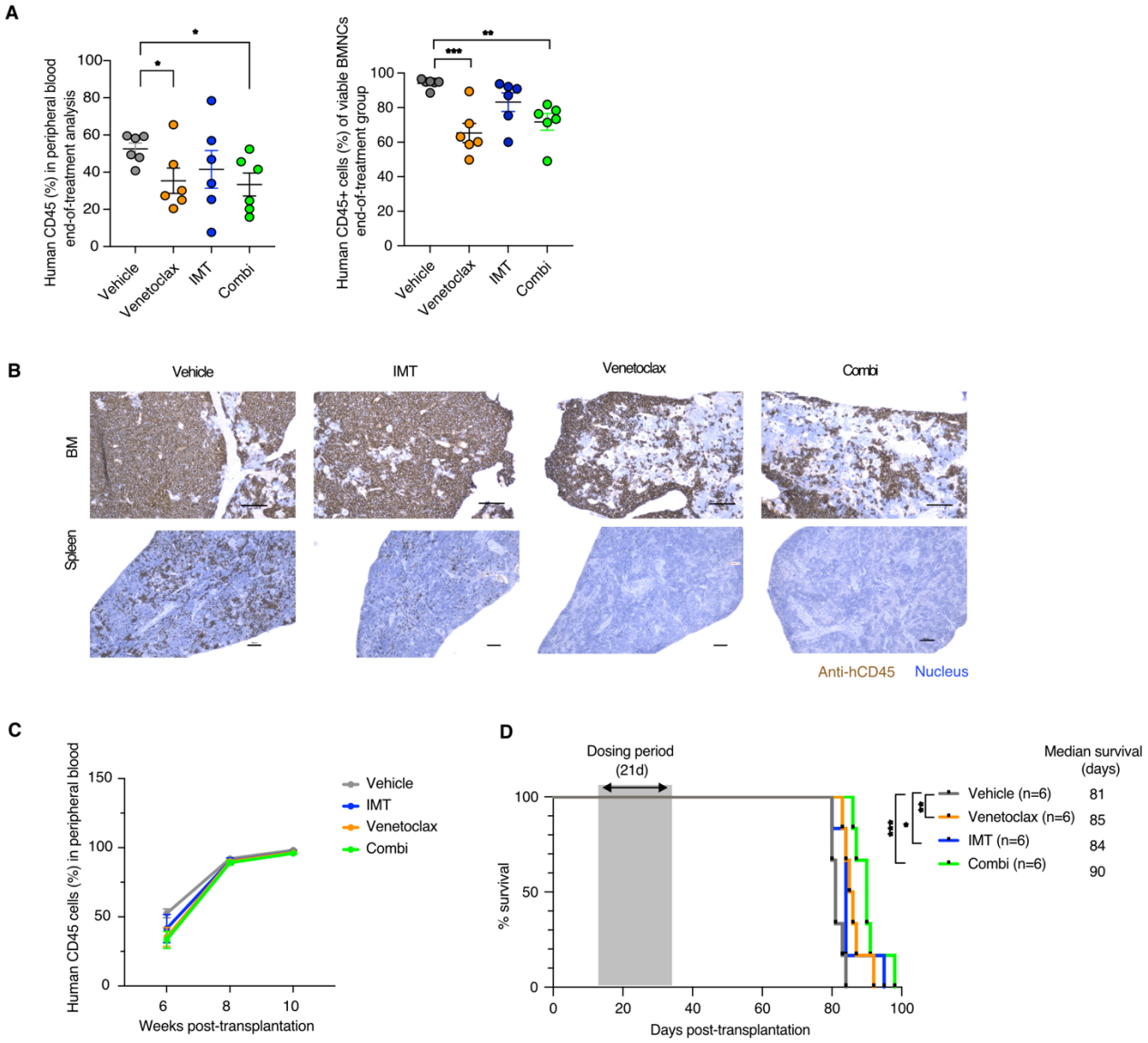
A
Human CD45 (%) in peripheral blood end-of-treatment analysis
Human CD45+ cells (%) of viable BMNCs end-of-treatment group
Vehicle
Venetoclax
IMT
Combi
B
Vehicle
IMT
Venetoclax
Combi
BM
Spleen
Anti-hCD45
Nucleus
C
Human CD45 cells (%) in peripheral blood
Weeks post-transplantation
D
Dosing period (21d)
% survival
Days post-transplantation
Median survival (days)
Vehicle (n=6) 81
Venetoclax (n=6) 85
IMT (n=6) 84
Combi (n=6) 90

726

727 **Figure 7. Leukemia progression induced by primary AML cells is inhibited by**
728 **venetoclax treatment**.

729 As in Fig. 5A, efficacy experiment outline: NSGS mice were transplanted with primary AML
730 splenocytes from PDX mice and were then treated with either vehicle, IMT, venetoclax, or a
731 combination of IMT and venetoclax (n=12 per treatment group). 8–12 h after the last dosing,
732 half of the mice (n=6/treatment group) were euthanized (end-of-treatment group) and the
733 other half were maintained for survival analysis. (**A**) Percentage of viable human CD45-
734 positive (hCD45+) cells in peripheral blood and bone marrow of treated mice (n=6 for each
735 treatment group), determined by flow cytometry. (**B**) Immunohistochemistry analysis of
736 hCD45+ cells on bone marrow and spleen tissue sections of treated mice (images are
737 representative from at least two mice per group). Scale bars represent 100 μM. (C) Peripheral
738 blood engraftment analysis of survival group. (**D**) Mice treated with single or a combination
739 of compounds showed prolonged survival in comparison to the vehicle-treated group.
740 Kaplan-Meier analysis shows the relative survival curve. *$P < 0.05$, **$P < 0.01$, and ***$p <$
741 0.001.